optica

Full-field broadband invisibility through reversible wave frequency-spectrum control

Luis Romero Cortés, ⓘ Mohamed Seghilani, ⓘ Reza Maram, ⓘ and José Azaña*

Institut National de la Recherche Scientifique—Énergie, Matériaux et Télécommunications (INRS-EMT), 800 de la Gauchetière Ouest, Suite 6900, Montréal, Québec H5A-1K6, Canada
*Corresponding author: azana@emt.inrs.ca

In recent years, a variety of interesting concepts have been proposed to enable the concealment of objects from detection or observation, including invisibility cloaking. For an object to remain truly transparent to an illumination wave, a cloak must restore the exact spatio-temporal profile of the wave, including both amplitude and phase variations across the entire illumination frequency spectrum, i.e., the *full field*. However, on the basis of their fundamental operating principles, present invisibility solutions force different frequency components of a broadband illumination wave to experience different phase variations, necessarily distorting the wave's temporal profile and making the cloaking device inherently visible. In this work, we propose a new conceptual approach to the problem, enabling the realization of full-field broadband invisibility, experimentally demonstrated here for the first time to the best of our knowledge. This involves a customized and reversible redistribution of the illumination frequency content, allowing the wave to propagate through the object of interest while preventing any interaction between the wave and the object. We report the experimental concealment of a broadband optical filter from detection with a phase-coherent light pulse of 500 GHz bandwidth, showing full restoration of the complex temporal and spectral profiles of the pulse.   © 2018 Optical Society of America under the terms of the OSA Open Access Publishing Agreement

1. INTRODUCTION

The last decade has witnessed a flourishing production of novel concepts and methods for concealing objects from detection, often referred to as invisibility cloaking [1–26]. Invisibility solutions operating over different regions of the electromagnetic spectrum, and even for waves of very different nature, such as acoustic and thermal waves, have been demonstrated. Spatial invisibility relies on specific transformations to redirect a wave around a prescribed zone in space, so that objects located therein avoid detection. Recently, methods for temporal invisibility—where a localized temporal event is concealed over a limited time period—were demonstrated [20–25]. These strategies have come a long way in achieving large operation bandwidths [7–18], so-called broadband invisibility. However, despite all this impressive progress, fundamental challenges remain unsolved. For a full concealment, an invisibility device must be able to restore the exact amplitude and phase profiles of the illumination wave (i.e., the full field), at its output. By fundamental design principles, current invisibility strategies are expected to introduce undesired relative phase variations among the different frequency components of a broadband illumination wave. Such phase distortion unavoidably alters the original illumination temporal profile [12–16]. Current invisibility approaches are thus vulnerable to detection by straightforward observation methods. For instance, a phase-coherent broadband illumination wave, e.g., a short pulse, will be severely distorted by the concealment or cloaking device, which could then be detected easily by an observer equipped with common phase-sensitive or temporal detection instruments [12–16]. Furthermore, recent in-depth studies, using full electromagnetic analysis, have additionally predicted that traditional spatial invisibility cloaks also induce further distortions directly across the energy spectrum profile of the broadband illumination wave [15].

These fundamental shortcomings are intrinsic to invisibility designs and strategies proposed to date, so that demonstration of full-field broadband invisibility, even for the simplest one-dimensional case (single illumination direction), remains a significant challenge [1,12–16]. It has been argued that fundamentally new concepts become necessary for the realization of this important paradigm [16,17,26]. In this paper, we propose a conceptually novel approach to the problem at hand, in the quest for realization of full-field broadband invisibility. For this purpose, we use reversible transformations of the illumination energy spectrum, allowing us to tailor at will the interaction between a wave and an object.

2. CONCEPT AND OPERATION PRINCIPLE

Figure 1(a) schematically illustrates the process of observation of an object through the distinct signature it imprints on the
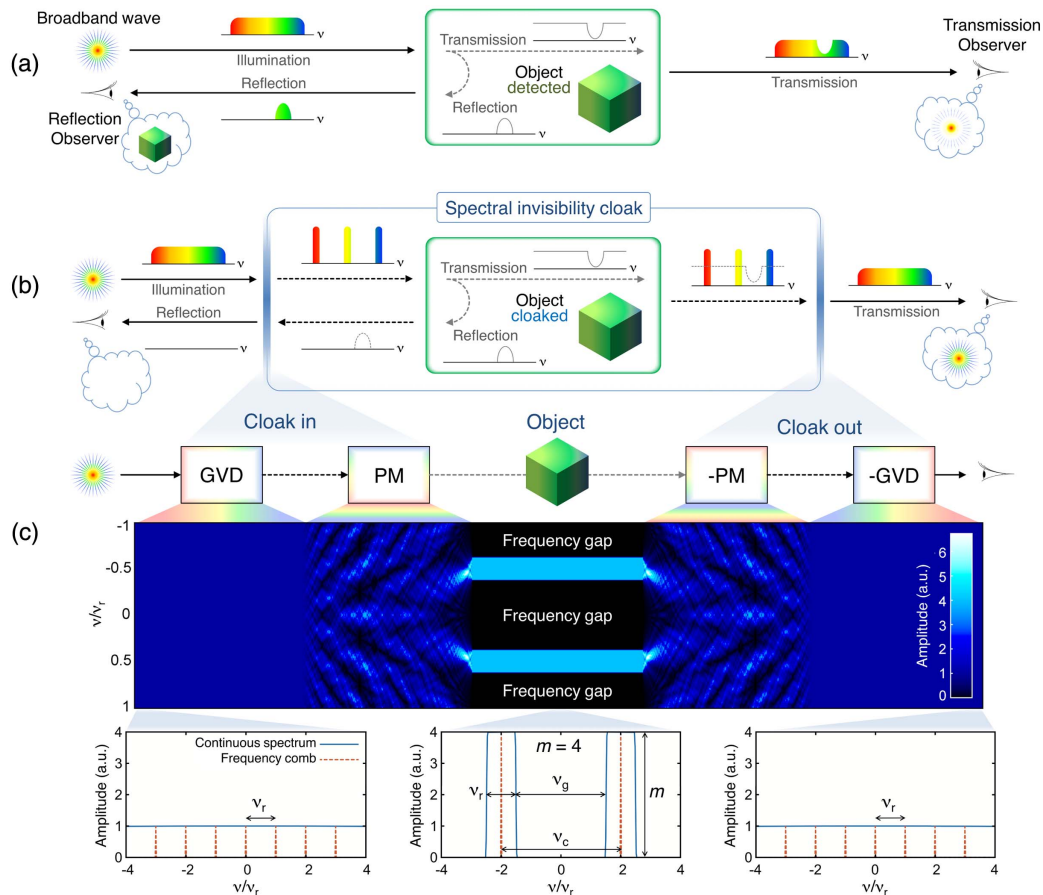
Fig. 1. Broadband invisibility cloaking through reversible wave-spectrum control. (a) Detection of a target (object) through the signature imprinted on the spectrum of a broadband wave (ν represents frequency). For simplicity of illustration, only backscattering (reflection) of the wave by the target is considered. (b) Concealing of the target by reversible transformations of the wave spectrum. (c) Numerical simulation of the proposed spectral cloak, operating on an illumination wave with a broadband continuous spectrum (solid blue curves, 2D representation) and a frequency comb (dashed red curves). Although the effect of PM occurs instantly, here it is depicted as a progressive process (2D representation) in order to reveal the intricate mechanism leading to the formation, and subsequent reversal, of the frequency gaps.

frequency spectrum of a broadband illumination wave. Such a signature can be observed either by direct frequency-domain measurements or through the observation of the associated changes in the temporal and/or spatial properties of the wave. The concept proposed here is based on redistributing the incoming wave energy toward frequency regions that will not be affected by the interaction with the object to be concealed (e.g., avoiding the object's absorption bands, scattering, resonances, etc.), through energy-preserving transformations. These transformations are designed to create a reversible *frequency gap* across the desired region(s) of the illumination spectrum [depicted in Fig. 1(b)]. The wave then propagates through the object without interacting with it, and subsequent application of the opposite transformations restores the wave spectrum to its exact original shape—in both amplitude and in phase—once the wave has cleared the object. This ensures that both the target and the cloaking device remain invisible to any observer, including broadband, phase-sensitive, or time-domain detection. Note that, although we refer to the proposed invisibility device as a "cloak" here, it should be emphasized that this newly proposed design is object-specific. In other words, a device implementing the reported technique would be designed to prevent any interaction between light and matter over a prescribed spectral region(s), so that, for effective

concealment, the frequency response of the targeted object must fit the operation bandwidth of the cloaking device.

Different specific implementations of this universal principle could be envisioned. Here we demonstrate a scheme based on linear phase transformations [27], inspired by the mathematical framework of temporal Talbot self-imaging [28–31]. In the reported method, a special realization of Talbot self-imaging is used to manipulate the frequency spectrum of an arbitrary wave, in contrast to the most conventional use of the phenomenon to modify the repetition rate of periodic signals [28]. Note that the temporal Talbot effect, in particular, the concept of a temporal Talbot array illuminator (T-TAI) [32], has been exploited previously for the implementation of temporal invisibility cloaks [22–24]. In a T-TAI, a train of short pulses is generated from a continuous temporal signal, e.g., a continuous-wave (CW) light beam. The specific implementation proposed here for spectral cloaking can be conceptually interpreted as the frequency-domain counterpart of a T-TAI, in which the energy of a broadband CW spectrum is redistributed into a train of narrow spectral peaks and the corresponding set of frequency gaps.

The proposed method is summarized in Fig. 1(c) (detailed illustrations in Fig. S1). For simplicity of explanation, let us first consider that the illumination wave exhibits a broadband

spectrum in the form of a phase-coherent periodic frequency comb—a set of equally spaced spectral lines with a linear phase relationship—with a free spectral range (FSR, the frequency separation between adjacent lines) ν_r. The associated temporal waveform is a periodic sequence of short pulses that completes a cycle every period, $t_r = \nu_r^{-1}$. We will afterwards extend this operation principle to the most general case of illumination with a broad continuous spectrum. As shown in Fig. 1(c), at the input of the cloaking device, the wave first propagates through a second-order group-velocity dispersive medium [33], such that its frequency components are not modified in intensity, but are linearly delayed with respect to each other, acquiring a spectral phase variation that shows a quadratic dependence with the frequency variable. For specific amounts of induced group-velocity dispersion (GVD), the original pulse train is self-imaged at the output of the dispersive medium (i.e., individual pulses are recovered with their exact initial shape), but repeating at a modified rate, i.e., with a pulse period that is divided by a natural number, m, with respect to the input one [28]. The associated comb-like power spectrum, however, remains unaltered, retaining its original FSR. This is known as the fractional temporal Talbot effect, and the relationship between the required dispersion, pulse period, and the factor m is given by the temporal Talbot condition [28,29]. The period-divided pulse train then acquires a deterministic pulse-to-pulse phase profile that can be calculated analytically [29,30] for any given m (see Supplement 1). If these phase variations are subsequently equalized through a temporal phase modulation (PM) mechanism, so that all the pulses in the train acquire the same phase [details in Fig. S1(a)], the corresponding FSR of the comb is increased m-fold [31], becoming

$$\nu_c = m\nu_r. \tag{1}$$

This effect is achieved exclusively through manipulations of the spectral and temporal phase profiles of the illumination wave; this way, the process preserves the entire wave energy, while redistributing it toward the desired frequency regions. This is key to the successful operation of the proposed cloak, since the illumination wave can be subsequently restored to its exact original state by simply applying the opposite phase transformations [depicted as -PM and -GVD in Fig. 1(c)]. Figure 1(c) shows a numerical simulation of the process with $m = 4$, where the predicted energy-preserving feature is confirmed.

Interestingly, when the described transformations are applied to a coherent broadband illumination wave with a purely continuous frequency spectrum, a periodic set of wideband *frequency gaps* is generated across the wave spectrum [additional details in Fig. S1(b)]. This corresponds to the most general situation where consecutive illumination pulses do not interact with each other in the cloaking device. In the case of a continuous spectrum (e.g., a single temporal pulse), the required phase transformations are the same ones described above for a periodic train of pulses; however, the values of m and ν_r can now be chosen arbitrarily to achieve the desired frequency gap bandwidth, set by

$$\nu_g = (m-1)\nu_r. \tag{2}$$

This makes the operation of the cloak independent of the properties (e.g., repetition rate) of the illumination wave (further clarifications below). As discussed above, the illumination wave can be subsequently restored to its exact original state through application of the opposite phase transformations. Figure 1(c) shows a numerical simulation of the process with $m = 4$, where

the original illumination spectrum is assumed to exhibit uniform intensity and phase distributions, although it should be noted that the process described for frequency gap generation can be generally produced on non-uniform illumination spectra (further discussions below). The predicted energy-preserving nature of the process is again confirmed in Fig. 1(c) for the case of broadband illumination with a continuous spectrum; this is an essential feature of the technique for exact recovery of the original illumination wave.

The proposed spectral concealment method relies entirely on linear wave transformations. As such, practical implementations could, in principle, be designed in any region of the electromagnetic spectrum, and for any wave-based platform (e.g., acoustics, matter waves, etc.). Here, we present an experimental demonstration using light pulses in the near-infrared.

3. MATERIALS AND METHODS

The illumination source used in the proof of concept reported here consists of a mode-locked laser (Menlo Systems FC1500-250-ULN) with a repetition rate of 250 MHz and an optical filter, used to select a 4 nm bandwidth around a central wavelength of 1554.5 nm (corresponding to ~500 GHz 3 dB bandwidth around 192.85 THz). These parameters are set to fit the specifications of the available time-domain measurement equipment. The resulting phase-coherent broadband frequency spectrum corresponds to a temporal pulse of ~1.4 ps.

As depicted in Fig. 2, the cloaking device consists of two sections of optical fiber—for implementation of the input and output GVD media—with equal dispersion magnitude and opposite signs, and two electro-optic phase modulators driven by a radio-frequency synthesizer.

A spool of 10 km of a standard single-mode fiber (Corning SMF-28) was used as the input dispersive section of the cloaking device, with a total second-order dispersion of 173 ps/nm
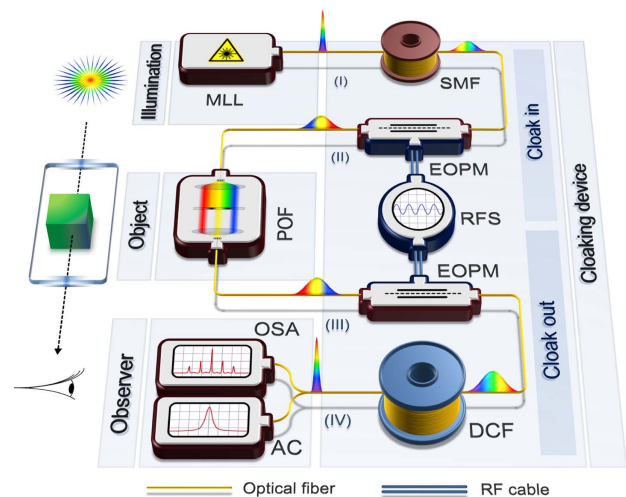

Fig. 2. Circuit layout of the reported experimental implementation of the spectral cloaking concept. Listed components: mode-locked laser (MLL), single-mode fiber (SMF), electro-optic phase modulator (EOPM), radio-frequency synthesizer (RFS), programmable optical filter (POF), dispersion-compensating fiber (DCF), optical spectrum analyzer (OSA), autocorrelator (AC). The labels (I)–(IV) mark key points in the setup to easily locate the measured signals that are reported in Figs. 3 and 4.

(corresponding to –222.6 ps^2/rad). The output dispersive section is matched to the input one by concatenating a spool of dispersion-compensating fiber (Corning DCM-20-SMF-C, designed to compensate for the dispersion of 20 km of SMF-28 at the working wavelength) with an additional 10 km spool of SMF-28. These dispersion values satisfy a fractional Talbot condition for $\nu_r = 19$ GHz and $m = 2$ (see Supplement 1). Note that this value of ν_r is 76 times higher than the repetition rate of the illumination laser; as such, the illumination repetition rate clearly does not satisfy a Talbot condition for the dispersion used in the cloak. Moreover, this amount of dispersion is insufficient to induce interference between any two consecutive pulses, thus ensuring no interaction among incoming pulses in the system.

Both electro-optic phase modulators (EOSpace, 40 GHz bandwidth LiNbO$_3$) are driven by a single-frequency tone at 19 GHz from a radio-frequency synthesizer (Agilent Technologies E8257D). The generated driving voltage corresponds to a first-order approximation of the $m = 2$ temporal Talbot phase sequence (as shown in Fig. S2). The applied driving voltage signal is aligned to the optical signal by a tunable optical delay line. Polarization controllers are used at the input of each modulator in order to maximize the modulation efficiency. Two radio-frequency amplifiers (OptiLab MD-50) are used to boost the output of the synthesizer before each modulation stage, in order to match the radio-frequency tone to the half-wave voltage of the phase modulators (see Fig. S2).

The object to be concealed is an optical filter (Finisar 4000S) with a linear frequency response consisting of a set of resonances (wideband "absorption" bands) spaced by 38 GHz, each with a 3 dB width of 17.5 GHz (detailed characterization in Fig. S3).

The observer is able to detect the output wave in both time and frequency domains. Frequency-domain measurements are performed with an optical spectrum analyzer (Apex Technologies AP2041B) with a frequency resolution of 2 GHz. Time-domain measurements are performed with an optical autocorrelator (Femtochrome FR-103XL); furthermore, an indirect reconstruction of the complex temporal envelope—including amplitude and phase profiles—is performed (details below).

4. RESULTS

The measured illumination spectrum is shown in Fig. 3(a). The spectral amplitude signature of the object is clearly observed in Fig. 3(b) when the phase modulators are not driven (cloak off). When the cloak is turned on, the designed phase transformations (GVD and PM in Fig. 1) produce the expected set of frequency gaps each with a bandwidth of $\nu_g = 19$ GHz, spaced apart by $\nu_c = 38$ GHz across the illumination spectrum [Fig. 3(c)]. A 3 dB increase in the spectral peak power level (corresponding to a linear factor of 2) is observed, in agreement with the expected conservation of energy (recall that the applied phase transformations simply redistribute the energy of the illumination wave across its frequency spectrum). The gaps induced prevent the interaction between the illumination wave and the object to be concealed, allowing the wave to propagate through the object unaltered. The wave can then be restored to its original state, following application of the inverted phase transformations (-PM and -GVD in Fig. 1) after clearing the object [Fig. 3(d)]. In this situation, an observer monitoring the output spectrum will detect the exact original illumination wave, as if neither the object nor
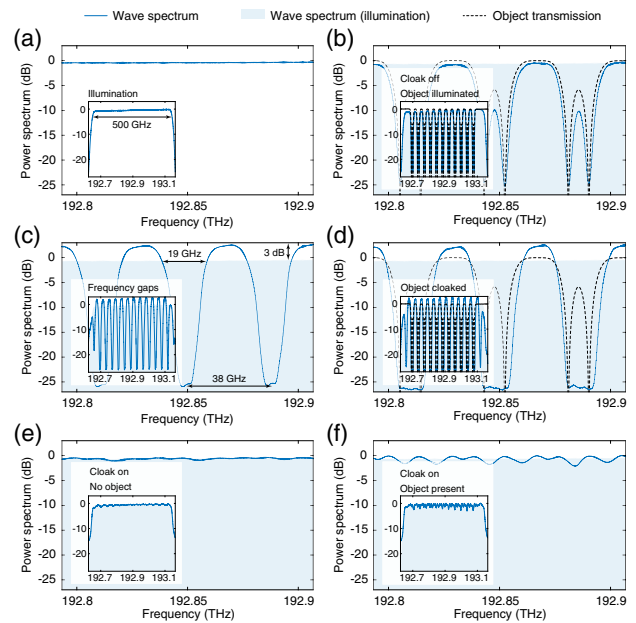

Fig. 3. Measured optical power spectra of the involved waves (normalized to the illumination spectral peak power). The transmission spectrum of the object to be concealed (linear optical filter) is shown for reference. Measurement points, as marked in Fig. 2, are indicated. (a) Illumination spectrum [Fig. 2(I)]. (b) Spectral amplitude signature of the object [Fig. 2(IV)]. (c) Frequency gaps induced in the illumination wave [Fig. 2(II)]. (d) Object's spectral response inserted in the frequency gaps [Fig. 2(III)]. (e) Output spectrum in the absence of the object when the cloak is on [Fig. 2(IV)]. (f) Output spectrum when the object is present and the cloak is on [Fig. 2(IV)].

the cloaking device were present [Figs. 3(e) and 3(f)]. The residual ripples on the recovered spectrum [Fig. 3(f)] are attributed to the fact that the object resonances are slightly wider than the frequency gaps generated across the illumination wave spectrum. For completeness, Fig. S4 shows a higher-resolution measurement of the frequency gap spectrum.

In order to demonstrate that the proposed cloak preserves the exact original full-field profile of the incoming illumination, we perform time-domain measurements of the propagating wave at the input and output of the cloak (Fig. 4). The measured temporal autocorrelation of the illumination wave [Fig. 4(a)] corresponds to that of a transform-limited pulse, i.e., with a flat spectral phase profile. This is evidenced by the good agreement between the measured autocorrelation trace of the illumination pulse and the expected trace for a transform-limited pulse, computed numerically from the power spectrum measured in Fig. 3(a), assuming a flat spectral phase distribution. When the cloak is off, the obtained output autocorrelation is significantly distorted, revealing the time-domain signature of the object [Fig. 4(b)]. In contrast, the wave propagates without any observable distortion when the cloak is turned on, independently of the presence or not of the object [Figs. 4(c) and 4(d)]. To quantify the similarity between the measured autocorrelation traces of the illumination and output waves, we calculate their cross-correlation coefficient, r (see Supplement 1). When the cloak is turned off and the object is illuminated, the similarity between the illumination and output pulses is found to be just over 13.6%. The operation of the cloak conceals both the object's signature and
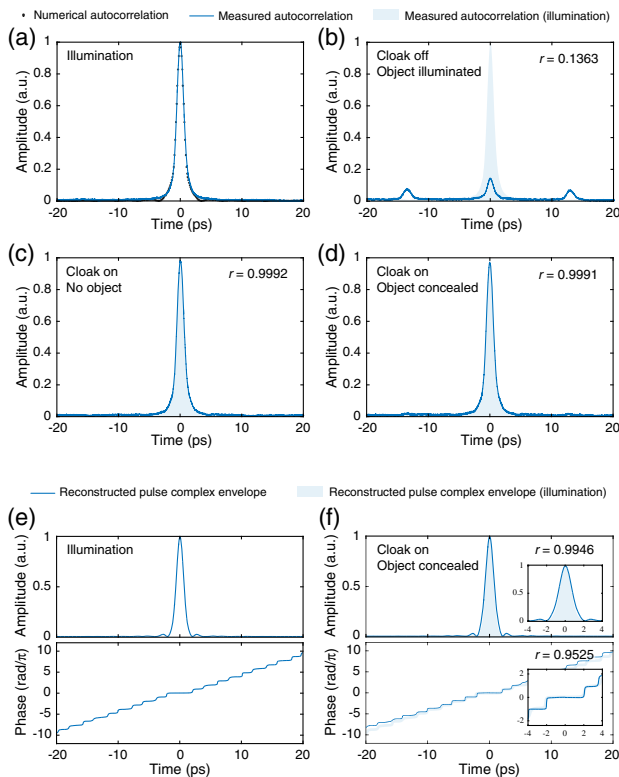
Fig. 4. Time-domain measurements of the involved waves. Measurement points, as marked in Fig. 2, are indicated. [(a)–(d)] Measured temporal autocorrelation traces. (a) Autocorrelation trace of the illumination wave [Fig. 2(I)]. (b) Temporal signature of the object when the cloak is off [Fig. 2(IV)]. (c) Autocorrelation trace when the object is not present and the cloak is on [Fig. 2(IV)]. (d) Autocorrelation trace when the object is present and the cloak is on [Fig. 2(IV)]. [(e)–(f)] Reconstruction of the complex temporal envelope of the involved waves. (e) Illumination pulse [Fig. 2(I)] and (f) output pulse with the object present and the cloak on [Fig. 2(IV)]. The estimated full width at half-maximum temporal duration of the pulse is ~1.4 ps.

the presence of the cloaking device itself, increasing the similarity between the illumination and output pulses to a value higher than 99.9%, regardless of the presence of the object.

Additionally, we perform an indirect reconstruction of the complex—amplitude and phase—temporal envelopes of the illumination and output pulses [Figs. 4(e) and 4(f), respectively] in the presence of the object, with the cloak on. The characterization method employed achieves reconstruction of the spectral phase profile of the wave under test through time-domain ultrafast optical differentiation [34] (see Supplement 1). The output pulse shows high similarity with the illumination pulse, quantified by a cross-correlation coefficient higher than 99% and 95% for the amplitude and phase profiles, respectively, confirming that the complex temporal envelope of the illumination wave is entirely preserved. It should be noted that the illumination wave still undergoes a temporal delay in propagating through the object and cloaking device, relative to the case of direct propagation from source to observer, potentially detectable through time-of-flight measurements [12–14]. However, as demonstrated here, the spectral cloak is designed to prevent any amplitude or phase distortion of the propagating wave, enabling a full-field recovery of the original illumination.

The proposed spectral cloak design also performs the desired operation for illumination waves with strong amplitude and phase variations along their frequency spectra (numerically confirmed in Fig. 5). From a practical viewpoint, such spectral variations could actually "encode" the signature of other surrounding objects. This could be related to previous works in temporal cloaking based on the T-TAI concept, where time gaps were introduced to a time-modulated (non-uniform) probe signal [23]. Since the proposed design has a symmetric architecture, the cloaking process is bidirectional. These two features would allow exchanging indistinctly the positions of the source and the observers, potentially enabling an observer to see behind the cloaked object without distortion, and without detecting the cloaking device [see illustration in Fig. 5(c)].

Another related, unique feature of the reversible wave-spectrum control method is its ability to selectively determine the specific frequency region(s) along which the wave–object interaction is permitted and/or avoided. For instance, the method could be crafted to conceal only a part of the frequency spectrum of the object, deliberately leaving the rest detectable, by strategically selecting the positions of the frequency gaps. This could be interpreted as selecting a range of colors of a multicolor object to be cloaked, while allowing the rest of the object to remain visible. Alternatively, several objects exhibiting different spectral interaction bands could be selectively concealed by properly tailoring the frequency response of the cloak. An experimental demonstration example is reported in Fig. 6, using an object with a spectral response comprising two separate absorption bands. The cloak is designed so that one of the object's absorption bands fits in a frequency gap, whereas the other one is located outside of the gaps; the band located at a frequency gap is cloaked (wave–object interaction prevented), whereas the one located outside of the gaps is detected (wave–object interaction allowed). This showcases the large degree of flexibility offered by the proposed concept to control the interaction between a wave and a specified target at will.

5. DISCUSSION AND CONCLUSION

As mentioned earlier, the reported methodology for redistributing the spectrum of a broadband wave into a periodic set of frequency gaps could be conceptually understood as a frequency-domain realization of a T-TAI [32]. In a T-TAI, a CW beam is focused into a train of short (ideally rectangular) optical pulses, following periodic PM of the input CW and dispersive propagation of the modulated signal, where both the PM profile and dispersive length are designed to induce a temporal Talbot effect. Such a concept has been exploited previously for temporal cloaking, namely, to hide information in the temporal gaps that are created in between the output short pulses [22–24]. The frequency gap generation process proposed here could then be interpreted as a spectral TAI (S-TAI), in that it produces a train of rectangular spectral peaks with high extinction ratios from a broadband wave. Similarly to the T-TAI case [22–24], the original broadband spectrum can be fully recovered by simply reverting the involved phase-only wave transformations. Nonetheless, it is important to note that from a mathematical viewpoint, there is a key difference between the implementations of the phase transformations involved in a T-TAI and those of the reported spectral cloak realization. For the formation of a T-TAI, a CW beam is first phase-modulated by a periodic Talbot phase sequence (i.e., a sequence of periodic phase steps satisfying the required Talbot condition; see Supplement 1), after which the phase-modulated wave
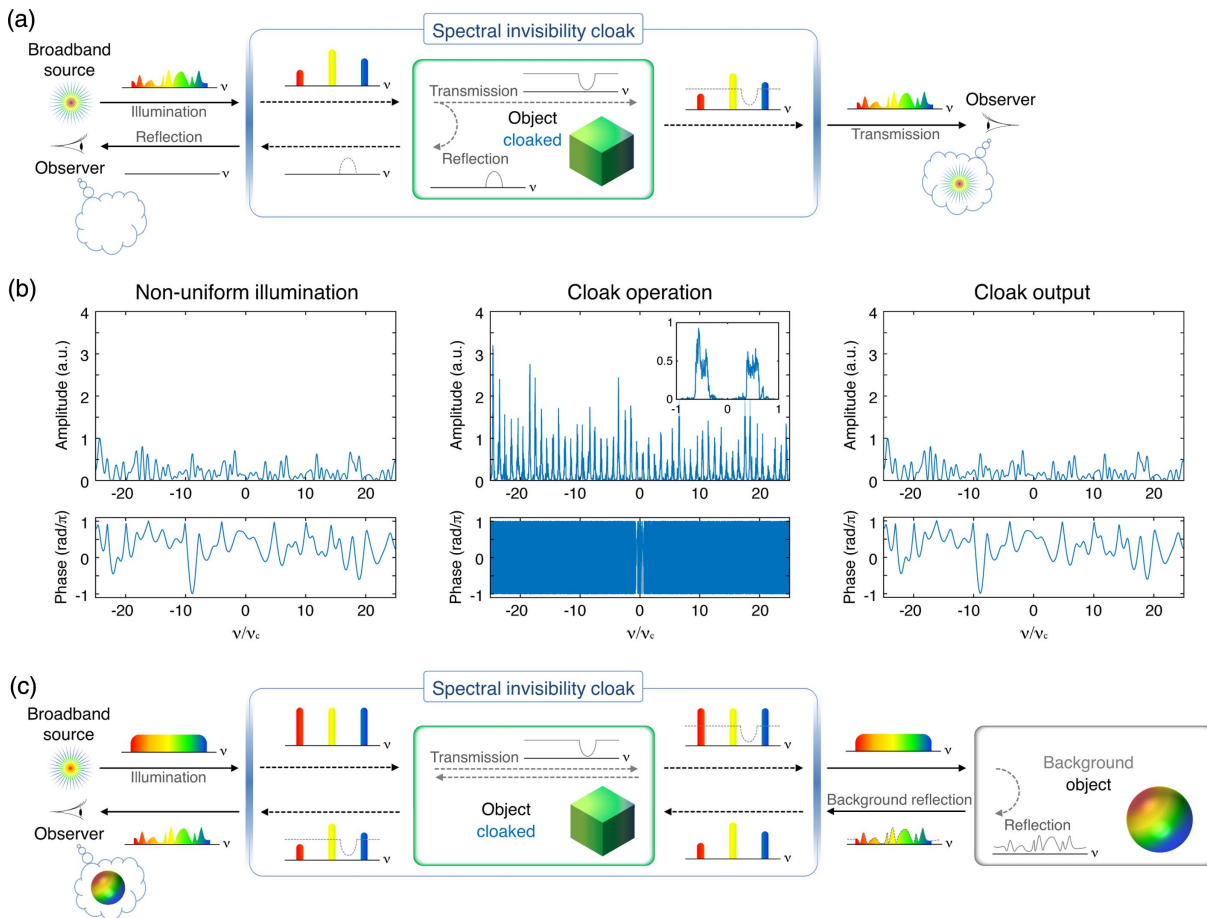
Fig. 5. Spectral cloaking with non-uniform broadband illumination. (a) Conceptual illustration of spectral cloaking of a target illuminated by a broadband wave with a non-uniform spectrum (ν represents frequency). (b) Numerical simulations of the spectral cloaking operation ($m = 2$) with a non-uniform illumination spectrum (see text for definitions of parameters). From left to right: non-uniform broadband illumination spectrum, frequency gaps resulting from the application of the cloak transformations, and reconstruction of the original illumination wave after reversal of the applied transformations. (c) Conceptual illustration of the detection of a target located in the background of a cloaked object.
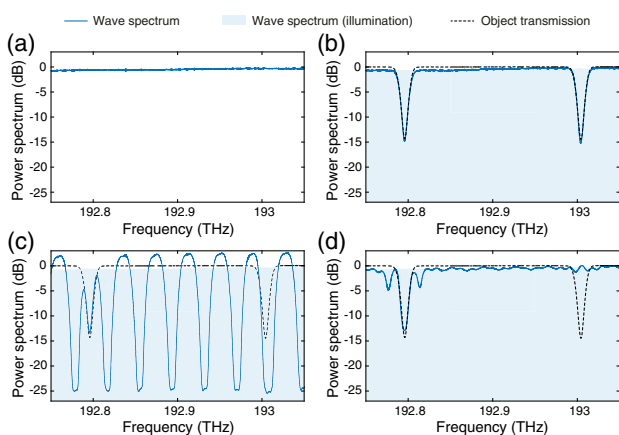

Fig. 6. Selective cloaking through spectrally tailored wave–object interaction. (a) Spectrum of the illumination wave. (b) Transmission spectrum of the object and the signature on the illumination wave when the cloak transformations are not applied. (c) Wave spectrum at the output of the first phase modulator [Fig. 2(b)], showing generation of spectral gaps. (d) Wave spectrum at the output of the cloaking device.

propagates through a certain GVD length, implementing a continuous quadratic phase filtering operation. In the reported spectral cloak implementation, the order of these operations is exchanged (GVD before PM); however, their definition remains unchanged, i.e., the first operation in the S-TAI (GVD) is still a continuous quadratic phase filter, whereas the second operation (PM) is a periodic step-like PM. A direct duality between the realizations of a T-TAI and an S-TAI would involve a direct exchange of the time and frequency domains, so that the S-TAI would consist of a first periodic step-like phase filter followed by a continuous quadratic temporal PM, as opposed to the method reported here. Our work demonstrates that it is possible to process a continuous spectrum (not necessarily periodic or discrete) through the Talbot effect; more precisely, we show that wave operations based on Talbot phase manipulations can be designed to affect the envelope of a coherent broadband wave, regardless of its repetition rate. Furthermore, from an implementation viewpoint, this finding implies that periodic or discrete spectral phase filters (potentially difficult to implement with good spectral resolution) are not an indispensable requisite for the implementation of the proposed spectral cloaking approach, and that the approach could still be implemented using a continuous quadratic spectral phase, such as that provided by widely available second-order dispersive media.

Our results confirm the unique potential of the proposed spectral cloaking concept to enable broadband invisibility with full-field restoration (i.e., recovering both the amplitude and phase variations of the illumination wave). Note that the optical filter used in the reported experiments is intended as a test object, engineered to probe a large spectral region of the demonstrated cloak; the purpose is to emulate the spectral response of a realistic object to be concealed in a practical implementation of the cloak. The GVD and PM transformations of the cloaking device could be designed to produce a sufficiently large gap bandwidth, ν_g, to accommodate the complete spectral response of the target object (known beforehand as a design specification of the cloak). It should be noted that a larger frequency gap bandwidth requires a lower GVD amount (see Supplement 1); however, a faster PM sequence would be required in this case, which translates into the need for faster electronic and electro-optical components. For the particular implementation based on Talbot effect reported here, the PM sequence used corresponds to a Talbot phase profile with $m = 2$, which can be well approximated by a sinusoidal function. However, the PM profiles resulting from Talbot conditions with arbitrary m factors are periodic sequences of phase steps (see Supplement 1). These can be practically implemented by an electronic arbitrary waveform generator. Furthermore, the modulation speed limitation, imposed by the available electronic bandwidth, could be relaxed through the use of alternative PM schemes, e.g., relying on nonlinear effects, such as cross-phase modulation in optical fibers [35]. In this context, it is also important to mention that, ideally, the GVD operation should apply uniformly to the entire probe wave bandwidth. As the illumination bandwidth increases, the higher-order dispersion terms of conventional dispersive media may become significant [33], potentially resulting in uncompensated phase distortion. However, available solutions exist for engineering the dispersion of an optical medium, so as to achieve a prescribed large value of the second-order term while suppressing the higher-order terms over wide frequency ranges. Some of these solutions include fiber Bragg gratings [36], specialty optical fibers [37,38], etc.

Solutions could potentially be envisioned to engineer the concept introduced here for application over large spatial regions and multiple directions, e.g., by replicating the specific design proposed here over a wide range of angles. As such, our findings could open a solid and promising new avenue toward practical realization of true (full-field) spatio-temporal broadband invisibility. Furthermore, the concept developed could be directly transferred to the transverse momentum domain of waves—so-called angular spectrum—by direct application of the well-known space-time duality of wave propagation [39]. This way, a method based on the reported concepts could be envisioned to cloak anisotropic spatial objects, i.e., objects sensitive to the specific direction in which they are illuminated, by only allowing light to shine the object in a controlled set of angles. Most importantly, the proposed fundamental principle for wave-spectrum control is not limited to the particular invisibility cloaking application reported here. More generally, this concept suggests a way to tailor at will the interaction between an incoming wave and a medium (i.e., a material, a device, a system, etc.), through reversible, energy-preserving transformations of the wave spectrum. To give just a basic example, the spectrum of a wave of interest could be reversibly transformed to avoid any interaction with undesired frequency bands of a medium or a system (e.g., high-absorption spectral regions), thus preventing loss and/or distortion. Such a capability could prove useful for many important applications, from enhanced control of linear and nonlinear wave dynamics to unprecedented opportunities in sensing, communications, and information processing.

It should also be noted that different sets of phase transformations, not necessarily based on the theory of Talbot effect, could be found to achieve the desired modification of a wave's frequency spectrum, not necessarily producing periodic frequency gaps. For instance, although the specific repetition rate and complex spectral profile of the probe wave do not affect the operation of the reported cloak design, an object illuminated by narrow-band or CW light would be detected; essentially, this particular cloak implementation requires an illumination bandwidth broader than ν_c for a frequency gap to be generated. Still, it is worth mentioning that in the absence of an object, the reported cloaking device would always remain invisible. Spectral cloaking of narrow-band illumination could be achieved by other phase transformations, e.g., simply by frequency shifting the illumination spectrum outside of the object's interaction band, and subsequently reversing the shift to the original illumination central frequency.

Finally, it is interesting to remark that the described methodology could be readily extended to any platform where control of the temporal and spectral phase distributions of waves is possible. Such operations are available over the entire electromagnetic spectrum [40], as well as for waves of very different nature, such as acoustic waves [41], thermal waves [42], matter waves [43,44], and the interesting case of single-photon quantum wavefunctions [45].

See Supplement 1 for supporting content.

REFERENCES

1. R. Fleury and A. Alù, "Cloaking and invisibility: a review," Prog. Electromagn. Res. **147**, 171–202 (2014).
2. G. Gbur, "Invisibility physics: past, present, and future," Prog. Opt. **58**, 65–114 (2013).
3. A. Alù and N. Engheta, "Achieving transparency with plasmonic and metamaterial coatings," Phys. Rev. E **72**, 016623 (2005).
4. U. Leonhardt, "Optical conformal mapping," Science **312**, 1777–1780 (2006).
5. J. B. Pendry, D. Schurig, and D. R. Smith, "Controlling electromagnetic fields," Science **312**, 1780–1782 (2006).
6. D. Schurig, J. J. Mock, B. J. Justice, S. A. Cummer, J. B. Pendry, A. F. Starr, and D. R. Smith, "Metamaterial electromagnetic cloak at microwave frequencies," Science **314**, 977–980 (2006).
7. L. Li and J. B. Pendry, "Hiding under the carpet: a new strategy for cloaking," Phys. Rev. Lett. **101**, 203901 (2008).

8. J. Valentine, J. Li, T. Zentgraf, G. Bartal, and X. Zhang, "An optical cloak made of dielectrics," Nat. Mater. **8**, 568–571 (2009).

9. R. Liu, C. Ji, J. J. Mock, J. Y. Chin, T. J. Cui, and D. R. Smith, "Broadband ground-plane cloak," Science **323**, 366–369 (2009).

10. A. Alù and N. Engheta, "Multifrequency optical invisibility cloak with layered plasmonic shells," Phys. Rev. Lett. **100**, 113901 (2008).

11. J. S. Choi and J. C. Howell, "Paraxial ray optics cloaking," Opt. Express **22**, 29465–29478 (2014).

12. U. Leonhardt and T. Tyc, "Broadband invisibility by non-Euclidean cloaking," Science **323**, 110–112 (2009).

13. D. A. B. Miller, "On perfect cloaking," Opt. Express **14**, 12457–12466 (2006).

14. J. S. Choi and J. C. Howell, "Paraxial full-field cloaking," Opt. Express **23**, 15857–15862 (2015).

15. C. Qian, R. Li, Y. Jiang, B. Zheng, H. Wang, Z. Xu, and H. Chen, "Transient response of a signal through a dispersive invisibility cloak," Opt. Lett. **41**, 4911–4914 (2016).

16. F. Monticone and A. Alù, "Invisibility exposed: physical bounds on passive cloaking," Optica **3**, 718–724 (2016).

17. J. S. Choi and J. C. Howell, "Digital integral cloaking," Optica **3**, 536–540 (2016).

18. S. Zang, C. Xia, and N. Fang, "Broadband acoustic cloak for ultrasound waves," Phys. Rev. Lett. **106**, 024301 (2011).

19. Y. Li, X. Shen, Z. Wu, J. Huang, Y. Chen, Y. Ni, and J. Huang, "Temperature-dependent transformation thermotics: from switchable thermal cloaks to macroscopic thermal diodes," Phys. Rev. Lett. **115**, 195503 (2015).

20. W. M. McCall, A. Favaro, P. Kinsler, and A. Boardman, "A spacetime cloak, or a history editor," J. Opt. **13**, 024003 (2011).

21. M. Fridman, A. Farsi, Y. Okawachi, and A. L. Gaeta, "Demonstration of temporal cloaking," Nature **481**, 62–65 (2012).

22. J. M. Lukens, D. E. Leaird, and A. M. Weiner, "A temporal cloak at tele-communication data rate," Nature **498**, 205–208 (2013).

23. J. M. Lukens, A. J. Metcalf, D. E. Leaird, and A. M. Weiner, "Temporal cloaking for data suppression and retrieval," Optica **1**, 372–375 (2014).

24. B. Li, X. Wang, J. Kang, Y. Wei, T. Yung, and K. K. Y. Wong, "Extended temporal cloak based on the inverse temporal Talbot effect," Opt. Lett. **42**, 767–770 (2017).

25. P. Y. Bony, M. Guasoni, P. Morin, D. Sugny, A. Picozzi, H. R. Jauslin, S. Pitois, and J. Fatome, "Temporal spying and concealing process in fibre-optic data transmission systems through polarization bypass," Nat. Commun. **5**, 4678 (2014).

26. M. Selvanayagam and G. V. Eleftheriades, "Experimental demonstration of active electromagnetic cloaking," Phys. Rev. X **3**, 041011 (2013).

27. J. van Howe and C. Xu, "Ultrafast optical signal processing based upon space-time dualities," J. Lightwave Technol. **24**, 2649–2662 (2006).

28. J. Azaña and M. A. Muriel, "Temporal self-imaging effects: theory and application for multiplying pulse repetition rates," IEEE J. Sel. Top. Quantum Electron. **7**, 728–744 (2001).

29. L. Romero Cortés, H. Guillet de Chatellus, and J. Azaña, "On the generality of the Talbot condition for inducing self-imaging effects on periodic objects," Opt. Lett. **41**, 340–343 (2016).

30. C. Rodríguez Fernández-Pousa, "On the structure of quadratic Gauss sums in the Talbot effect," J. Opt. Soc. Am. A **34**, 732–742 (2017).

31. L. Romero Cortés, R. Maram, H. Guillet de Chatellus, and J. Azaña, "Noiseless spectral amplification of optical frequency combs," in *Conference on Lasers and Electro-Optics (CLEO)*, San Jose, California (2017), paper STu4I.

32. C. Rodríguez Fernández-Pousa, R. Maram, and J. Azaña, "CW-to-pulse conversion using temporal Talbot array illuminators," Opt. Lett. **42**, 2427–2430 (2017).

33. A. M. Weiner, *Ultrafast Optics* (Wiley, 2009).

34. J. Azaña, Y. Park, T.-J. Ahn, and F. Li, "Simple and highly sensitive optical pulse-characterization method based on electro-optic spectral signal differentiation," Opt. Lett. **33**, 437–439 (2008).

35. R. Maram and J. Azaña, "Spectral self-imaging of time-periodic coherent frequency combs by parabolic cross-phase modulation," Opt. Express **21**, 28824–28835 (2013).

36. R. Kashyap, *Fiber Bragg Gratings* (Academic, 2009).

37. K. Thyagarajan, R. K. Varshney, P. Palai, A. K. Ghatak, and I. C. Goyal, "A novel design of a dispersion compensating fiber," IEEE Photon. Technol. Lett. **8**, 1510–1512 (1996).

38. S. Yang, Y. Zhang, L. He, and S. Xie, "Broadband dispersion-compensating photonic crystal fiber," Opt. Lett. **31**, 2830–2832 (2006).

39. B. H. Kolner, "Space-time duality and the theory of temporal imaging," IEEE J. Quantum Electron. **30**, 1951–1963 (1994).

40. J. D. Jackson, *Classical Electrodynamics* (Wiley, 1998).

41. W. M. Robertson, C. Baker, and C. B. Bennett, "Slow group velocity propagation of sound via defect coupling in a one-dimensional acoustic band gap array," Am. J. Phys. **72**, 255–257 (2004).

42. A. Fornieri and F. Giazotto, "Towards phase-coherent caloritronics in superconducting circuits," Nat. Nanotechnol. **12**, 944–952 (2017).

43. A. D. Cronin, J. Schmiedmayer, and D. E. Pritchard, "Optics and interferometry with atoms and molecules," Rev. Mod. Phys. **81**, 1051–1129 (2009).

44. L. Deng, E. W. Hagley, J. Denschlag, J. E. Simsarian, M. Edwards, C. W. Clark, K. Helmerson, S. L. Rolston, and W. D. Phillips, "Temporal, matter-wave-dispersion Talbot effect," Phys. Rev. Lett. **83**, 5407–5411 (1999).

45. P. Kolchin, C. Belthangady, S. Du, G. Y. Yin, and S. E. Harris, "Electro-optic modulation of single photons," Phys. Rev. Lett. **101**, 103601 (2008).